






Cite this: *Chem. Commun.*, 2024, 60, 4906

Received 3rd March 2024,  
Accepted 9th April 2024

DOI: 10.1039/d4cc01016g

rsc.li/chemcomm

# Photocatalytic aerobic $\alpha$ -oxygenation of amides to imides using a highly durable decatungstate tetraphenylphosphonium salt†

Chen Gu, Takafumi Yatabe,  Kazuya Yamaguchi  and Kosuke Suzuki \*

**Decatungstate is a potent photocatalyst for hydrogen atom transfer (HAT) but faces degradation issues when using a typical tetra-*n*-butylammonium salt. Herein, we employed tetraphenylphosphonium as a counteranion to yield a highly durable and efficient HAT photocatalyst, enabling  $\alpha$ -oxygenation of amides to their corresponding imides using  $O_2$  as an oxidant.**

Hydrogen atom transfer (HAT) reactions, which involve homolytic cleavage of C–H bonds by hydrogen abstractors, are notable methods for the direct C–H functionalization of various organic molecules without prefunctionalization (directing group) and high acidity of C–H bonds in substrates.<sup>1,2</sup> Photocatalysts play a crucial role in facilitating HAT as an eco-friendly method.<sup>2,3</sup> Decatungstate ( $[W_{10}O_{32}]^{4-}$ , **W10**), a type of metal oxide cluster (namely, polyoxometalate),<sup>4</sup> is a widely employed HAT photocatalyst.<sup>3,5</sup> Experimental and theoretical studies have elucidated its mechanism as a photocatalyst.<sup>6</sup> Upon UV light irradiation, **W10** undergoes intramolecular ligand-to-metal charge transfer (LMCT) from  $O^{2-}$  to  $W^{6+}$ , forming a singlet excited state. This excited state promptly decays to a relaxed state, **wO**, which exhibits remarkable reactivity and can react with substrates *via* both HAT and single-electron-transfer (SET) mechanisms. Exploiting the robust HAT capability of **W10**, various synthetic reactions, such as oxygenation, dehydrogenation, and C–X (X = C, N, S, F, Si) bond formation, have been possible.<sup>2,5,7–9</sup> Typically, **W10** is employed as a tetra-*n*-butylammonium (TBA) salt (TBAW10) in photocatalytic organic reactions because of its solubility in organic solvents and availability from chemical reagent suppliers. However, photo-excited **W10** undergoes HAT not only with substrates but also with its counteranion, TBA, decomposing TBA cations during

photocatalytic reactions and causing various issues (though these are rarely mentioned in the literature)—decreased solubility and activity of TBAW10, difficulties in its reusability, and impurity formation in its products.<sup>10</sup>

To address the issues, we propose using a counteranion with a structure that has a higher bond dissociation energy (BDE) than the alkyl group of TBA. Because the BDE of the C–H bond of benzene (113 kcal mol<sup>−1</sup>) is substantially higher than those of the C–H bonds of alkyl groups (95–100 kcal mol<sup>−1</sup>),<sup>11</sup> aryl groups in cations may provide higher resistance to HAT by **W10** photocatalysis while retaining solubility in organic solvents. Specifically, a tetraphenylphosphonium (TPP) cation, which possesses no structures other than aryl groups, is inherently more chemically and thermally stable than quaternary alkylammonium cations. Thus, employing TPP as the counteranion of **W10** promises considerable durability improvement compared with conventional alkylammonium cations.

Imides are essential structures in natural compounds and pharmaceuticals.<sup>12</sup> Conventional methods for imide synthesis involve the acylation of amides with acyl halides,<sup>13</sup> aldehydes,<sup>14</sup> esters,<sup>15</sup> thioesters,<sup>16</sup> and acid anhydrides.<sup>17</sup> Nevertheless, these methods require stoichiometric amounts of reactants, resulting in a high environmental impact. Therefore, the direct synthesis of imides through  $\alpha$ -oxygenation of amides has garnered considerable attention<sup>18</sup> because of its reduced number of reaction steps, use of various readily available amide structures, and the potential for using  $O_2$  as an oxidant under mild conditions, particularly when combined with photocatalysis. Several photocatalytic systems have been explored for this reaction; however, there are still challenges, such as limited substrate scope, excessive oxidant usage, and prolonged reaction time (Table S1, ESI†).<sup>12,18</sup>

In this study, we synthesized a highly durable and efficient **W10** photocatalyst as a TPP salt (TPPW10, TPP<sub>4</sub>[W<sub>10</sub>O<sub>32</sub>]). Notably, TPPW10 demonstrated efficient photocatalysis for direct imide synthesis *via*  $\alpha$ -oxygenation of several amides using  $O_2$  as an oxidant (Fig. 1). By employing TPP as a counteranion, cation degradation by **W10** during the photocatalytic

Department of Applied Chemistry, School of Engineering, The University of Tokyo, 7-3-1 Hongo, Bunkyo-ku, Tokyo 113-8656, Japan.

E-mail: ksuzuki@appchem.t.u-tokyo.ac.jp

† Electronic supplementary information (ESI) available: Detailed experimental methods and spectroscopic data. CCDC 2336024. For ESI and crystallographic data in CIF or other electronic format see DOI: <https://doi.org/10.1039/d4cc01016g>



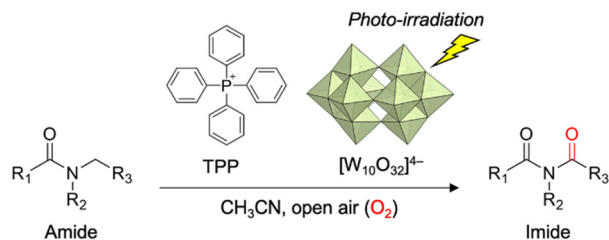


Fig. 1 Direct imide synthesis via photocatalytic aerobic  $\alpha$ -oxygenation of amides using highly durable and efficient TPPW10.

reaction was circumvented, and TPPW10 exhibited substantial activity for the  $\alpha$ -oxygenation compared with typical photocatalysts. Further, we demonstrated that TPPW10 can be readily recovered after the reaction and reused without loss of its high activity.

Synthesis of TPPW10 was conducted *via* the cation exchange of an *in situ* formed sodium salt of W10 by reacting with excess amounts of TPP bromide in a hot aqueous solution (see ESI† for details). The obtained TPPW10 was characterized by electrospray ionization-mass spectrometry (ESI-MS), infrared (IR), UV-vis,  $^1\text{H}$  nuclear magnetic resonance (NMR), and  $^{31}\text{P}$  NMR spectroscopies. In the ESI-MS spectrum in acetonitrile ( $\text{CH}_3\text{CN}$ ), two sets of signals were observed at  $m/z$  2193.4 and 4047.0 that are attributable to  $[\text{TPPW}_{10}\text{O}_{32}]^{2+}$  and  $[\text{TPPW}_{10}\text{O}_{32}]^+$ , respectively (Fig. S1, ESI†). The IR spectrum exhibited characteristic absorption bands derived from W–O–W and W=O bonds of W10 (Fig. S2, ESI†). The UV-vis spectrum in  $\text{CH}_3\text{CN}$  exhibited an absorption band of O-to-W LMCT ( $\lambda_{\text{max}} = 324 \text{ nm}$ ) (Fig. S3, ESI†), and it was confirmed that the TPP cation has no absorption in the region above 300 nm (Fig. S4, ESI†). The  $^1\text{H}$  NMR spectrum exhibited signals ascribed to the aryl groups of TPP, and the  $^{31}\text{P}$  NMR spectrum exhibited a single peak attributed to the P atom in TPP (Fig. S5, ESI†). Moreover, single crystals suitable for the X-ray diffraction study were obtained by recrystallization in a mixed solvent of  $\text{CH}_3\text{CN}$  and diethyl ether, and the TPPW10 structure was unambiguously determined using single-crystal structural analysis (Fig. S6, ESI†).

We employed TPPW10 as a photocatalyst for aerobic  $\alpha$ -oxygenation of amides to synthesize their corresponding imides. Initially, 1-methyl-2-pyrrolidone (**1a**) was used as a model substrate for the reaction (Table 1). With 0.7-mol% TPPW10, **1a** was oxygenated and selectively converted to the corresponding imide product, *N*-methylsuccinimide (**2a**), in 83% yield by photoirradiation from a Xe lamp ( $\lambda > 350 \text{ nm}$ ) for 4 h under an air atmosphere in  $\text{CH}_3\text{CN}$  (Table 1, entry 1; Fig. S7, ESI†). The reaction also proceeded using LED ( $\lambda = 365, 405 \text{ nm}$ ) instead of a Xe lamp (Table 1, entries 3 and 4). When using TBAW10, which is a widely used TBA salt of W10, the yield of **2a** was 73% (Table 1, entry 5). The reaction did not proceed when performed in the dark or under an Ar atmosphere (Table 1, entries 6 and 7), indicating that the photoexcitation of W10 and  $\text{O}_2$  is essential for the reaction. In addition, oxygenation did not proceed when using sodium tungstate ( $\text{Na}_2\text{WO}_4$ ; Table 1, entry 8). Other polyoxometalate photocatalysts,  $\text{TBA}_3[\alpha\text{-PW}_{12}\text{O}_{40}]$  and  $\text{TBA}_4\text{H}[\gamma\text{-PV}_2\text{W}_{10}\text{O}_{40}]$ ,<sup>19</sup> were ineffective for the reaction (Table 1,

Table 1 The  $\alpha$ -oxygenation of **1a** to **2a** using various photocatalysts<sup>a</sup>

Entry	Photocatalyst	Conv. (%)		Yield (%)	
		1a	2a	3a	
1	TPPW10	> 99	83	1	
2	TPPW10 (reuse)	> 99	80	4	
3 <sup>a</sup>	TPPW10 (LED, 365 nm)	> 99	70	1	
4 <sup>b</sup>	TPPW10 (LED, 405 nm)	> 99	73	1	
5	TBAW10	> 99	73	1	
6	TPPW10 (dark)	< 1	< 1	< 1	
7	TPPW10 (Ar)	< 1	< 1	< 1	
8	$\text{Na}_2\text{WO}_4$	2	< 1	< 1	
9	$\text{TBA}_3[\alpha\text{-PW}_{12}\text{O}_{40}]$	4	2	< 1	
10	$\text{TBA}_4\text{H}[\gamma\text{-PV}_2\text{W}_{10}\text{O}_{40}]$	10	2	1	
11	Benzophenone	43	18	2	
12	Xanthone	18	6	< 1	
13	Anthraquinone	23	9	1	
14	2-Chloroanthraquinone	14	8	2	
15	Eosin Y	17	8	1	
16	$\text{TiO}_2$ (P25)	32	9	7	

<sup>a</sup> Reaction conditions: **1a** (0.6 mmol), photocatalyst (0.7 mol%),  $\text{CH}_3\text{CN}$  (3 mL), open air, and 4-h photoirradiation using Xe lamp ( $\lambda > 350 \text{ nm}$ ). Conversions and yields were determined by gas chromatography analysis using *N*-methylphthalimide as an internal standard. LED ( $\lambda = 365 \text{ nm}$ ). <sup>b</sup> LED ( $\lambda = 405 \text{ nm}$ ).

entries 9 and 10). Notably, TPPW10 showed considerably higher activity than organic molecular HAT photocatalysts, such as benzophenone, xanthone, anthraquinone, 2-chloroanthraquinone, and eosin Y (Table 1, entry 1 vs. entries 11–15). Although  $\text{TiO}_2$  is a frequently-used heterogeneous inorganic photocatalyst, it showed lower **1a** conversion and **2a** yield compared to those by TPPW10, and byproduct **3a** was generated in almost the same amount as **2a** (Table 1, entry 16).

To investigate the structures of TPP cation and W10 anion after the photocatalytic  $\alpha$ -oxygenation of **1a** under the conditions described in Table 1, TPPW10 was recovered as a powder by adding the concentrated reaction solution to ethyl acetate, a poor solvent for TPPW10, followed by filtration and vacuum drying (Fig. S8, ESI†). The  $^1\text{H}$  NMR spectrum of the recovered TPPW10 exhibited signals in the range of 7.6–8.0 ppm, attributable to the aryl groups of TPP, and other signals derived from the oxidation of TPP were unobserved (Fig. 2a). The  $^{31}\text{P}$  NMR spectrum showed only a single signal at 23.3 ppm, attributable to the P atom in TPP (Fig. 2b). These results confirm that the TPP cation structure was maintained after the photocatalytic reaction. Using IR spectroscopy, we also confirmed that the W10 anion structure was maintained after the photocatalytic reaction (Fig. 2c and Fig. S9, ESI†). Further, the ESI-MS spectrum of the recovered catalyst exhibited signals attributable to TPPW10 ( $m/z$  2194.0 and 4047.5 for  $[\text{TPPW}_{10}\text{O}_{32}]^{2+}$  and  $[\text{TPPW}_{10}\text{O}_{32}]^+$ , respectively; Fig. S10, ESI†). Notably, the recovered TPPW10 can be reused for imide synthesis without loss of its high photocatalytic activity; **1a** was converted to **2a** in 80% yield using the recovered TPPW10 (0.7 mol%) after 4-h photoirradiation (Table 1, entry 2).



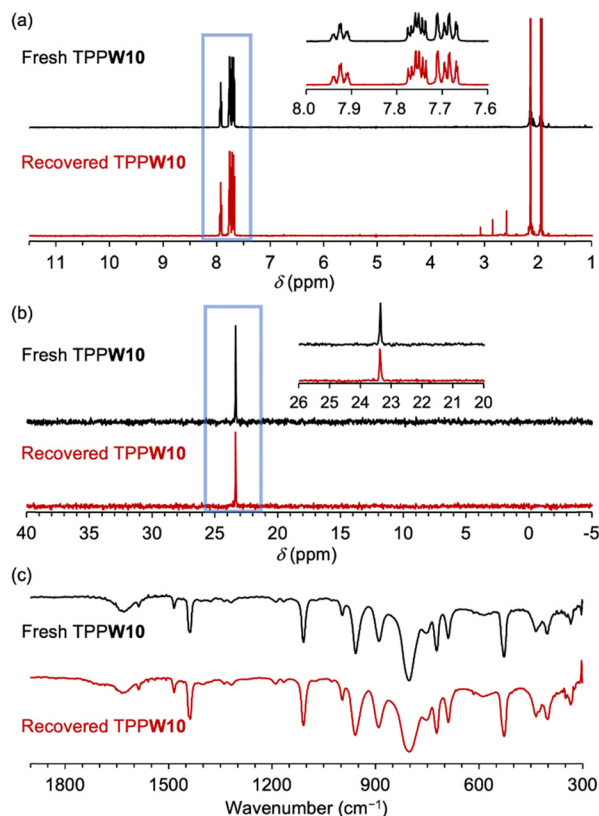


Fig. 2 (a)  $^1\text{H}$ , (b)  $^{31}\text{P}$  nuclear magnetic resonance spectra ( $\text{CD}_3\text{CN}$ ), and (c) infrared spectra of the fresh and recovered TPPW10 after the photocatalytic aerobic  $\alpha$ -oxygenation of **1a**.

Although we also attempted to recover TBAW10 *via* the same procedure used for TPPW10 after the photocatalytic reaction of **1a**, a sticky sample was formed, and the catalyst was difficult to be recovered by filtration. When we performed a reuse experiment for the photocatalytic reaction of **1a** using the sticky catalyst, the yield of **2a** became notably lower (45% yield) than the reaction using fresh TBAW10 (73% yield). To analyze the structure of TBA cations after the reaction, we performed the photocatalytic  $\alpha$ -oxygenation of **1a** using TBAW10 in deuterated acetonitrile ( $\text{CD}_3\text{CN}$ ) and measured the  $^1\text{H}$  NMR spectrum of the reaction solution after a 4-h reaction. The  $^1\text{H}$  NMR spectrum showed that the peaks of the alkyl groups of TBA completely disappeared (Fig. S11, ESI $^\dagger$ ), indicating TBA degradation.

Next, we investigated the reaction mechanism by performing several experiments. When a radical scavenger, 2,2,6,6-tetramethylpiperidine 1-oxyl, was added to the reaction solution, the conversion of **1a** and yield of **2a** considerably decreased (Table S2, ESI $^\dagger$ ), suggesting that the reaction proceeded *via* radical generation. To identify the oxygen source in the reaction,  $^{18}\text{O}$ -isotope labeling experiments were performed (Fig. 3), and the products were analyzed by gas chromatography (GC) and GC-mass spectrometry (GC-MS). When **1a**  $\alpha$ -oxygenation was performed using TPPW10 photocatalysis under an  $^{18}\text{O}_2$  atmosphere, **2a** was obtained in 81% yield. The formation of  $^{18}\text{O}$ -labeled **2a** with an  $^{18}\text{O}$  content of 88% was revealed *via* GC-MS analysis using the ratio of peak intensities at  $m/z$  115 ( $^{18}\text{O}$ -labeled **2a**) and  $m/z$  113

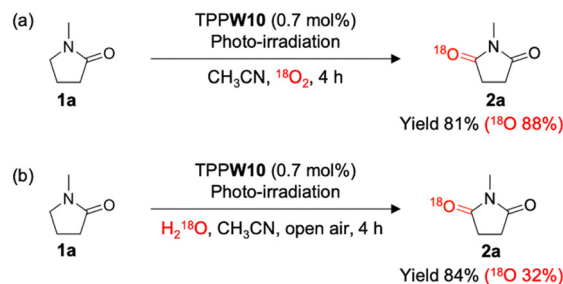


Fig. 3  $^{18}\text{O}$  labeling experiments for the photocatalytic aerobic  $\alpha$ -oxygenation of **1a** using TPPW10: (a) under an  $^{18}\text{O}_2$  atmosphere and (b) in the presence of  $\text{H}_2^{18}\text{O}$  (59 mg). Reaction conditions: **1a** (0.6 mmol), TPPW10 (0.7 mol%),  $\text{CH}_3\text{CN}$  (3 mL), and 4-h photoirradiation using Xe lamp ( $\lambda > 350$  nm).

(**2a**) (Fig. S12, ESI $^\dagger$ ). In addition, when **1a**  $\alpha$ -oxygenation was performed in the presence of  $\text{H}_2^{18}\text{O}$  (59 mg, 5 equivalents with respect to **1a**) under an air atmosphere, GC-MS analysis revealed the formation of  $^{18}\text{O}$ -labeled **2a** with an  $^{18}\text{O}$  content of 32%, indicating that  $\text{H}_2\text{O}$  also acted as the oxygen source of the reaction (minor path; Fig. S13a, ESI $^\dagger$ ). Even when the amount of  $\text{H}_2^{18}\text{O}$  was increased (294 mg, 15 equivalents with respect to **1a**), the  $^{18}\text{O}$  content remained almost unchanged (Fig. S13b, ESI $^\dagger$ ). Therefore, the major oxygen source of this reaction is  $\text{O}_2$  rather than  $\text{H}_2\text{O}$ .

Based on the above results, we proposed a plausible reaction mechanism (Fig. 4). A carbon-centered radical was generated through the HAT process on the  $\alpha$ -position of **1a** by the photoexcited W10. In contrast, it has been reported that SET on **1a** by photoexcited W10 does not occur. $^{20}$  The generated carbon-centered radical on **1a** reacted with  $\text{O}_2$  to form a peroxy radical ( $\text{R-OO}^\bullet$ ), which further reacted with **1a** or the reduced W10 to form hydroperoxide, finally resulting in the formation of **2a** (major path A). Another plausible reaction path involves the reaction with  $\text{H}_2\text{O}$  (minor path B): the carbon-centered radical through HAT on **1a** reacted with the photoexcited W10 through SET to form an iminium cation, which underwent nucleophilic attack by  $\text{H}_2\text{O}$  to form hydroxylated **1a** and then further oxidized to form **2a**.

Finally, we investigated the substrate scope of the TPPW10-catalyzed system (Fig. 5). The reactions of pyrrolidone derivatives with methyl, ethyl, and phenyl groups substituting the N atoms proceeded efficiently to yield their corresponding imides

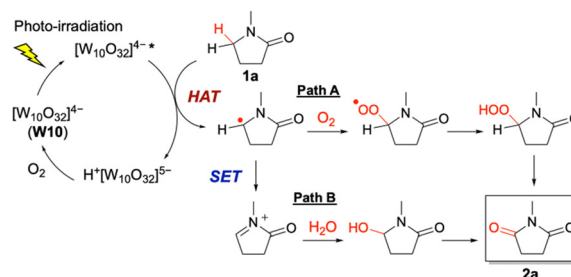
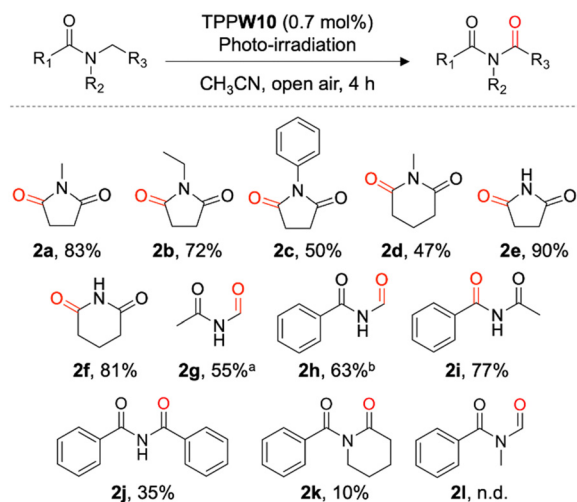


Fig. 4 Proposed reaction mechanism for the photocatalytic aerobic  $\alpha$ -oxygenation of **1a** to **2a** using W10 *via* hydrogen atom transfer (HAT, major path A) and single electron transfer (SET, minor path B).







**Fig. 5** Substrate scope for photocatalytic aerobic  $\alpha$ -oxygenation of **1a** using TPPW10. Reaction conditions: substrate (0.6 mmol), TPPW10 (0.7 mol%), CH<sub>3</sub>CN (3 mL), open air, and 4-h photoirradiation using Xe lamp ( $\lambda > 350$  nm). Yields were determined by gas chromatography using *N*-methylphthalimide as internal standard (n.d. = not detected). <sup>a</sup> 5 h, <sup>b</sup> 6 h.

(**2a–2c**). In this process, cyclic methylene moieties were selectively oxidized. This was applicable even when the ring size of the cyclic amides increased; for example, a corresponding imide (**2d**) was selectively obtained from 1-methyl-2-piperidone. Not only cyclic tertiary amides but also noncyclic amides can be applied to the reaction; for example, the reaction of *N*-methylethanamide yielded the corresponding imide **2g**. Notably, using the TPPW10-catalyzed system, various secondary cyclic, noncyclic, and benzylic amides can also be converted to their corresponding imides (**2f–2j**). However, this system was not effective to obtain imide products **2k** and **2l** owing to dealkylation during the photocatalytic reactions.

In conclusion, we synthesized a highly durable and reactive decatungstate tetraphenylphosphonium salt (TPPW10), which efficiently promoted the photocatalytic aerobic  $\alpha$ -oxygenation of various tertiary and secondary amides to their corresponding imides. TPPW10 showed significantly higher activity for the photocatalytic aerobic  $\alpha$ -oxygenation of imides than previously reported photocatalytic systems. Further, TPPW10 can be easily recovered after the photocatalytic reaction and reused for the photocatalytic reaction without notable loss of its high activity; the structures of both the TPP cation and W10 anion were maintained in the recovered catalyst.

This study was supported in part by JST FOREST (JPMJFR213M), JSPS KAKENHI (22H04971), and the JSPS Core-to-Core program. We would like to thank Dr Li and Mr Hachimura for their contribution in the preliminary experiments.

## Conflicts of interest

There are no conflicts to declare.

## Notes and references

- J. M. Mayer, *Acc. Chem. Res.*, 2011, **44**, 36.
- (a) L. Capaldo, L. L. Quadri and D. Ravelli, *Green Chem.*, 2020, **22**, 3376; (b) H. Cao, X. Tang, H. Tang, Y. Yuan and J. Wu, *Chem. Catal.*, 2021, **1**, 523; (c) L. Capaldo, D. Ravelli and M. Fagnoni, *Chem. Rev.*, 2022, **122**, 1875; (d) K. Ohmatsu and T. Ooi, *Nat. Synth.*, 2023, **2**, 209.
- (a) A. Albini and M. Fagnoni, *Green Chem.*, 2004, **6**, 1; (b) D. Ravelli, D. Dondi, M. Fagnoni and A. Albini, *Chem. Soc. Rev.*, 2009, **38**, 1999.
- (a) M. T. Pope, *Heteropoly and Isopoly Oxometalates*, Springer, Berlin, 1983; (b) C. L. Hill and C. M. Prosser-McCarthy, *Coord. Chem. Rev.*, 1995, **143**, 407; (c) R. Neumann, *Prog. Inorg. Chem.*, 1998, **47**, 317; (d) D.-L. Long, R. Tsunashima and L. Cronin, *Angew. Chem., Int. Ed.*, 2010, **49**, 1736; (e) C. Streb, *Dalton Trans.*, 2012, **41**, 1651; (f) S.-S. Wang and G.-Y. Yang, *Chem. Rev.*, 2015, **115**, 4893; (g) A. Misra, K. Kozma, C. Streb and M. Nyman, *Angew. Chem., Int. Ed.*, 2020, **59**, 596; (h) J. M. Cameron, G. Guillemot, T. Galambos, S. S. Amin, E. Hampson, K. M. Haidaraly, G. N. Newton and G. Izzet, *Chem. Soc. Rev.*, 2022, **51**, 293.
- (a) D. Ravelli, M. Fagnoni, T. Fukuyama, T. Nishikawa and I. Ryu, *ACS Catal.*, 2018, **8**, 701; (b) K. Suzuki, N. Mizuno and K. Yamaguchi, *ACS Catal.*, 2018, **8**, 10809; (c) M. D. Tzirakis, I. N. Lykakis and M. Orfanopoulos, *Chem. Soc. Rev.*, 2009, **38**, 2609; (d) C. Li, C. Gu, K. Yamaguchi and K. Suzuki, *Nanoscale*, 2023, **15**, 15038.
- (a) C. Tanielian, *Coord. Chem. Rev.*, 1998, **178**, 1165; (b) D. C. Duncan, T. L. Netzel and C. L. Hill, *Inorg. Chem.*, 1995, **34**, 4640; (c) V. D. Waele, O. Poizat, M. Fagnoni, A. Bangno and D. Ravelli, *ACS Catal.*, 2016, **6**, 7174.
- (a) C. Tanielian, K. Duffy and A. Jones, *J. Phys. Chem. B*, 1997, **101**, 4276; (b) D. M. Schultz, F. Lévesque, D. A. DiRocco, M. Reibarkh, Y. Ji, L. A. Joyce, J. F. Dropinski, H. Sheng, B. D. Sherry and I. W. Davies, *Angew. Chem., Int. Ed.*, 2017, **56**, 15274; (c) G. Laudadio, S. Govaerts, Y. Wang, D. Ravelli, H. F. Koolman, M. Fagnoni, S. W. Djuric and T. Noël, *Angew. Chem., Int. Ed.*, 2018, **57**, 4078.
- J. G. West, D. Huang and E. J. Sorensen, *Nat. Commun.*, 2015, **6**, 10093.
- (a) G. Laudadio, Y. Deng, K. van der Wal, D. Ravelli, M. Nuño, M. Fagnoni, D. Guthrie, Y. Sun and T. Noël, *Science*, 2020, **369**, 92; (b) P. J. Sarver, N. B. Bissonnette and D. W. C. MacMillan, *J. Am. Chem. Soc.*, 2021, **143**, 9737; (c) P. J. Sarver, V. Bacauanu, D. M. Schultz, D. A. DiRocco, Y. Lam, E. C. Sherer and D. W. C. MacMillan, *Nat. Chem.*, 2020, **12**, 459; (d) D. Ravelli, S. Protti and M. Fagnoni, *Acc. Chem. Res.*, 2016, **49**, 2232.
- (a) T. Yamase, N. Takabayashi and M. Kaji, *J. Chem. Soc., Dalton Trans.*, 1984, 793; (b) L. P. Ermolenko and C. Giannotti, *J. Chem. Soc., Perkin Trans.*, 1996, **2**, 1205.
- (a) Y.-R. Luo, *Comprehensive Handbook of Chemical Bond Energies*, CRC Press, Boca Raton, 2007; (b) S. J. Blanksby and G. B. Ellison, *Acc. Chem. Res.*, 2003, **36**, 255; (c) W. Xie, Z. Gao, W. P. Pan, D. Hunter, A. Singh and R. Vaia, *Chem. Mater.*, 2001, **13**, 2979.
- J. Sperry, *Synthesis*, 2011, 3569.
- M. Klinge, H. Cheng, T. M. Zabriskie and J. C. Vederas, *J. Chem. Soc., Chem. Commun.*, 1994, 1379.
- L. Wang, H. Fu, Y. Jiang and Y. Zhao, *Chem. – Eur. J.*, 2008, **14**, 10722.
- M. B. Andrus, W. Li and R. F. Keyes, *Tetrahedron Lett.*, 1998, **39**, 5465.
- F. Wang, H. Liu, H. Fu, Y. Jiang and Y. Zhao, *Adv. Synth. Catal.*, 2009, **351**, 246.
- D. Davidson and H. Skovronek, *J. Am. Chem. Soc.*, 1958, **80**, 376.
- (a) J. C. Gramain, R. Remuson and Y. Troin, *J. Chem. Soc., Chem. Commun.*, 1976, 194; (b) J. W. Pavlik and S. Tantayanon, *J. Am. Chem. Soc.*, 1981, **103**, 6755; (c) C. Mei, Y. Hu and W. Lu, *Synthesis*, 2018, 2999; (d) S. Liu, Z. Dong, Z. Zang, C. Zhou and G. Cai, *Org. Biomol. Chem.*, 2024, **22**, 1205.
- C. Li, K. Suzuki, N. Mizuno and K. Yamaguchi, *Chem. Commun.*, 2018, **54**, 7127.
- S. Angioni, D. Ravelli, D. Emma, D. Dondi, M. Fagnoni and A. Albini, *Adv. Synth. Catal.*, 2008, **350**, 2209.

